Warm turbulence in the Boltzmann equation

Davide Proment* and Miguel Onorato
Dipartimento di Fisica Generale, Università degli Studi di Torino, Via Pietro Giuria 1, 10125 Torino, Italy and INFN, Sezione di Torino, Via Pietro Giuria 1, 10125 Torino, Italy

Sergey Nazarenko
Mathematics Institute, The University of Warwick, Coventry, CV4-7AL, UK

Pietro Asinari
Dipartimento di Energetica, Politecnico di Torino, Corso Duca degli Abruzzi 24, 10129 Torino, Italy
(Dated: March 29, 2011)

We study the single-particle distributions of three-dimensional hard sphere gas described by the Boltzmann equation. We focus on the steady homogeneous isotropic solutions in thermodynamically open conditions, i.e. in the presence of forcing and dissipation. We observe nonequilibrium steady state solution characterized by a warm turbulence, that is an energy and particle cascade superimposed on the Maxwell-Boltzmann distribution. We use a dimensional analysis approach to relate the thermodynamic quantities of the steady state with the characteristics of the forcing and dissipation terms. In particular, we present an analytical prediction for the temperature of the system which we show to be dependent only on the forcing and dissipative scales. Numerical simulations of the Boltzmann equation support our analytical predictions.

PACS numbers: 47.27.Gs, 05.70.Ln, 47.70.Nd

Three-dimensional fluid turbulence is characterized by an energy cascade process whose concept was introduced by Richardson in 1922 and developed by Kolmogorov in 1941 [1, 2]. The idea is that if one injects energy at some scale, creating eddies, then those eddies may interact and create smaller and smaller eddies up to the dissipation scale. The result is the famous power-law Kolmogorov spectrum which corresponds to a constant flux of energy from large to small scales.

Some years later, in 1965 [3], Zakharov found that dispersive weakly nonlinear wave systems, e.g. surface gravity waves, may exhibit a very similar phenomenology as fluid turbulence, i.e. a constant flux of energy towards small scales, a *direct cascade*. Besides ocean waves [4], these cascades have been studied in a large number of weakly nonlinear systems such as internal waves [5], nonlinear optics [6], Bose-Einstein condensation [7–9], magnetohydrodynamics [10]. Such regime, valid for weak nonlinearity, is now known as *weak wave turbulence* and the power-law flux carrying states are called Kolmogorov-Zakharov (KZ) spectra. The extraordinary fact is that the KZ solutions corresponding to the turbulent cascades are found to be exact analytical solutions of a *wave kinetic equation* which describes the evolution of the wave spectrum. The wave kinetic equation has a structure that resembles the classical Boltzmann equation: the evolution of the distribution is driven by a collision integral which conserves mass, momentum and energy.

Keeping in mind such an analogy, our aim is to address in the present Letter the following fundamental questions. Let us consider a gas whose single-particle distribution evolution is described by the Boltzmann equation and suppose that we inject in the system particles with a specific energy and remove those that reach an energy larger/smaller than a preselected threshold. How does the distribution function change with respect to the thermodynamic equilibrium solution? How the temperature and chemical potential will be affected by the presence of forcing and dissipation?

In order to answer we will first consider numerical simulations of the Boltzmann equation in the homogeneous and isotropic case and then present an argument based on dimensional analysis that allows us to explain the numerical results and make some predictions on the steady nonequilibrium properties of the system. Our starting point is the homogeneous, forced and damped Boltzmann equation

$$\begin{aligned} &\frac{\partial n_1}{\partial t} = I_{coll} + F - D, \quad \text{with} \\ &I_{coll} = \int_{-\infty}^{+\infty} W_{12}^{1'2'} \left[n_1' n_2' - n_1 n_2 \right] d\mathbf{v}_2 d\mathbf{v}_1' d\mathbf{v}_2', \end{aligned} \tag{1}$$

where $n_i \equiv n(\mathbf{x}, \mathbf{v}_i, t)$ is the single-particle distribution function and primes denote particles after the collision. We have included a source term F and a sink D which will be specified once the numerics are discussed. As we consider elastic collisions, the general way to express W is

$$W_{12}^{1'2'} = \sigma\, \delta(\mathbf{v}_1 + \mathbf{v}_2 - \mathbf{v}_1' - \mathbf{v}_2')\, \delta(E_1 + E_2 - E_1' - E_2'), \tag{2}$$

with $E_i = |\mathbf{v}_i|^2/2$ being the kinetic energy per unit mass. The δ-functions assure conservation of the total momen-

tum and the total kinetic energy. In this Letter, we consider the three-dimensional rigid sphere gas (σ is independent of $\mathbf{v}$) in isotropic conditions.

In absence of forcing and dissipation any initial condition will relax to the Maxwell-Boltzmann (MB) distribution

$$n_{MB}(E) = n_0\, e^{-\frac{E+\mu}{T}} = A\, e^{-\frac{E}{T}}, \tag{3}$$

where $A \equiv n_0\, e^{-\frac{\mu}{T}}$ with μ and T the chemical potential and temperature of the system respectively. This equipartition mechanism, consequence of the H-theorem, has been checked as a benchmark of our numerical code. In order to consider an open system we have then included forcing and dissipation written in E-space. The forcing term is constant in time and has the role of injecting particles with energies narrowly concentrated around some value E_f, i.e. $F(E) = F$ if $|E - E_f| < \delta_f$ and zero otherwise, where F is a positive constant. The dissipation term is implemented as a filter which removes, at each iteration time, energy and particles outside of the domain $(E_{\min}, E_{\max})$, i.e. $D(E) = 0$ if $E \in (E_{\min}, E_{\max})$ and $D(E) = -\infty$ otherwise. In such conditions, a dimensional analysis shows that (1) may have also solutions characterized by a constant flux of energy and mass which corresponds to the KZ solutions. Indeed, the particle flux η and the energy flux ϵ can be estimated as:

$$\begin{aligned} \eta &= 2\pi \int_0^E \frac{\partial n}{dt}\, E^{1/2} dE \sim n^2 E^{7/2} \\ \epsilon &= 2\pi \int_0^E \frac{\partial n}{dt}\, E^{3/2} dE \sim n^2 E^{9/2}. \end{aligned} \tag{4}$$

Assuming that one of the fluxes is constant trough energy scales, we can immediately derive the KZ solutions $n_\eta \sim E^{-7/4}$ and $n_\epsilon \sim E^{-9/4}$ [11].

In our simulations the computational domain is uniformly discretized in 501 points having $\Delta E = 1$ and the initial distribution is $n(E, t = 0) = 0$. We first consider the case characterized by $E_{\min} = 5$, $E_{\max} = 250$ and the forcing located at energies between 35 and 37. Numerical results for the final steady states evaluated for three different forcing amplitudes, $F = 10^{-4}, 10^{-5}, 10^{-6}$, are presented in Fig. 1. Independently of the forcing, a stationary distribution is reached in the simulations, implying the existence of a flux from the forcing region to the boundaries of the domain. The steady solutions of our simulation do not appear to be very far from the Maxwell-Boltzmann distribution (3), which corresponds to a straight line in a lin-log coordinates. It is clear from the plot that the only consequence of increasing the forcing rate is to shift upwards the curves, leaving unchanged the slopes. This is the first indication that the temperature of the system remains constant, independently of the forcing. We can also compute, as a function of time, the average energy per particle ρ_E/ρ_M, with $\rho_M = 2\pi \int n(E)\, E^{1/2}\, dE$ and $\rho_E = 2\pi \int n(E)\, E^{3/2}\, dE$.

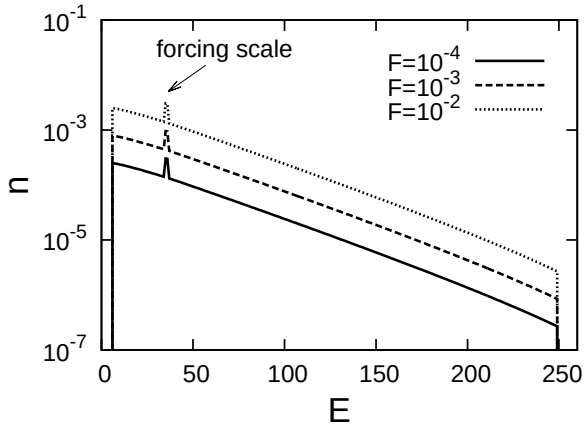

FIG. 1: Final steady states of the Boltzmann equation (1) obtained for different values of the forcing amplitude F. Axes are in lin-log coordinates. $E_{\min} = 5$, $E_{\max} = 250$ and $E_f = 35 - 37$.

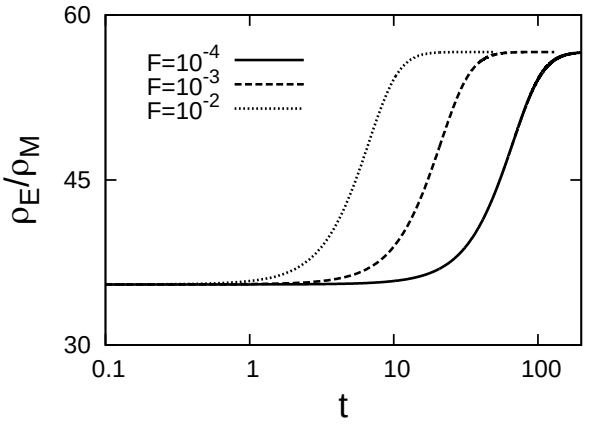

FIG. 2: Time evolution of the average energy per particle for different forcing amplitudes. Axes are in log-lin coordinates. $E_{\min} = 5$, $E_{\max} = 250$ and $E_f = 35 - 37$.

As shown in Fig. 2, for large times this quantity reaches a unique value for the three simulations considered. We recall that for a pure MB distribution such ratio is proportional to 3/2 the temperature of the system.

We have not observed KZ solutions in our simulations. The reason is that the interactions are non-local in scales, as already pointed out in [12]: the collision integral does not converge for such solutions. Moreover, the energy and particle flux directions, [13], associated to such solutions, are opposite to the one predicted by the Fjørtoft argument which imposes that the energy should have a direct cascade, i.e. from low to high energies, while particle an inverse one [14].

As shown in Fig. 1, we observe distributions not far from the thermodynamic equilibrium (3) solution. However, we are in a forced and dissipated situation and let us assume the existence of a small but finite flux correction

"living on top" of the Maxwell-Boltzmann distribution. This behavior, named *warm cascade*, has already been observed in other physical systems [6, 15] and is characterized by constant flux cascades perturbing the thermodynamic equilibrium distribution. Mathematically, we assume that

$$n = n_{MB}\,(1+\tilde{n}), \tag{5}$$

with $\tilde{n}$ the deviations with respect to the MB distribution which are responsible for the fluxes; note that not necessarily $\tilde{n}$ is small with respect to one. If we plug such *ansatz* in the equations for the fluxes (4) we obtain

$$\begin{aligned} \eta &= c_1\, n_{MB}^2\, \tilde{n}\,(2+\tilde{n})\, E^{7/2} \\ \epsilon &= c_2\, n_{MB}^2\, \tilde{n}\,(2+\tilde{n})\, E^{9/2}, \end{aligned} \tag{6}$$

where c_1 and c_2 are two constants which cannot be determined through dimensional analysis. The term n_{MB}^2, corresponding to the unperturbed MB distribution, does not give any contribution because it is not responsible for any net flux.

Our aim is to relate the macroscopic properties of the system with the forcing and dissipation rates. From our numerical computation we observe that, as we get closer to the cut-off scales ($E_{\min}$ and $E_{\max}$), deviations from a pure MB distribution becomes more relevant. Consequently, $\tilde{n}$ becomes of the order one for $E = E_{\min}$ or $E = E_{\max}$ and therefore from (6) we have

$$\begin{aligned} \eta &= c_1\, A^2\, e^{-\frac{2\,E_{\min}}{T}}\, E_{\min}^{7/2} \\ \epsilon &= c_2\, A^2\, e^{-\frac{2\,E_{\max}}{T}}\, E_{\max}^{9/2}, \end{aligned} \tag{7}$$

where we have redefined the constant c_1 and c_2. We now verify the above relations through the direct computation of the Boltzmann equation. In Fig. 3 we show the dependence of A on the fluxes for three simulations previously described (Fig. 1). Supposing to use as temperature of the system the simple relation coming from the MB distribution $T = 2\rho_E/3\rho_M$, we can observe in Fig. 3 (and its inset) that A scales as the square root of the incoming fluxes for fixed dissipative scales $E_{\min}$ and $E_{\max}$. From the numerics we can estimate, by a fit, the constants c_1 and c_2 whose values are reported in the figure.

We are now able to predict the dependence of the temperature on the forcing and the dissipative scales. Assuming that they are widely separated, that is $E_{\min} \ll E_f \ll E_{\max}$, we have $\epsilon = \eta\, E_f$. Then from equations (7) we get

$$T = \frac{2\,(E_{\max} - E_{\min})}{\frac{9}{2}\ln E_{\max} - \frac{7}{2}\ln E_{\min} - \ln E_f + c_3} \tag{8}$$

with $c_3 = \ln(c_2/c_1)$. The temperature of the system does not depend on the incoming fluxes but only on the forcing and dissipative scales; this is consistent with results of the numerical simulations presented in Fig. 1 and 2.

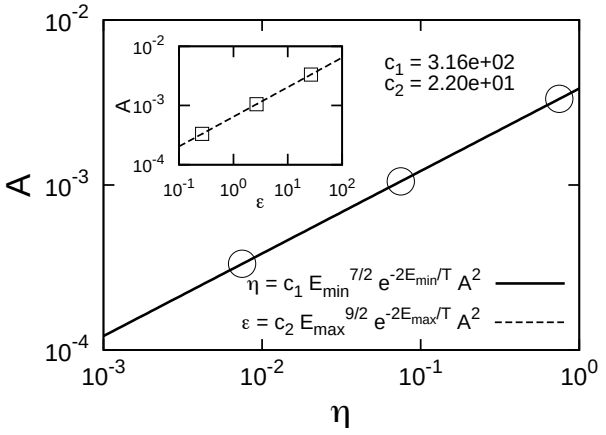

FIG. 3: A as a function of the fluxes. Circles (and squares in the inset) correspond to the numerical simulation results. The continuous and dashed lines are the predictions (7) where the temperature, $T = 2\rho_E/3\rho_M$, has been defined using the pure MB distribution. The values of the constant c_1 and c_2, shown in the plot, are found by a fit.

We can check the validity of prediction (8) by considering different simulations of the isotropic Boltzmann equation (1) changing the forcing and dissipative scales. Before entering in the details, we emphasize that our predictions are based on a dimensional argument and c_1 and c_2, which define c_3, can only be measured *via* numerical computations. In our simulations we have observed that, as $E_{\min}$, E_f and $E_{\max}$ changes, c_1 and c_2 assumes different values. This may be related to the fact that we are considering the hypothesis that the particle flux is all dissipated at low energy scales and all energy flux at high ones, that is $E_{\min} \ll E_f \ll E_{\max}$. This is not always verified in the numerical simulations due to finiteness of the computational domain. In our numerical simulations we have measured an upper and lower bound for our constants leading to $-4.21 \le c_3 \le -1.05$. This interval includes the analytical prediction $c_3 = 2\ln(2/9)$ obtained using a *diffusion approximation model* in the limit $E_{\min} \ll T \ll E_{\max}$ presented in [14].

In Fig. 4 we show the comparison between the estimation of the temperature from (8) and the numerical simulation varying the low energy dissipation scale $E_{\min}$. The incoming flux, the forcing and the high energy dissipative scale have been kept fixed to the respective values of $F = 10^{-3}$, $E_f = 36$, $\delta_f = 1$, $E_{\max} = 250$. The dashed and the solid line in the figure are the predictions obtained with $c_3 = -1.05$ and $c_3 = -4.21$, respectively. The agreement between the temperature prediction and the computation is satisfactory.

In Fig. 5 we present the behavior of the temperature as a function of the high energy cut-off scale $E_{\max}$, with $F = 10^{-3}$, $E_{\min} = 5$ and $E_f = 36$, $\delta_f = 1$. The comparison between our estimation (8) and the numerics is very good.

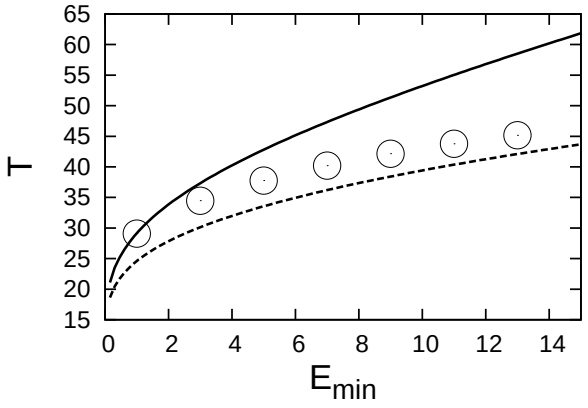

FIG. 4: Temperature as a function of the low energy cut-off $E_{\min}$, keeping fixed $F = 10^{-3}$, $E_f = 36$, $\delta_f = 1$ and $E_{\max} = 250$. Circles represent the results from numerical computations. The continuous and dashed lines are the prediction (8) for different values of c_3.

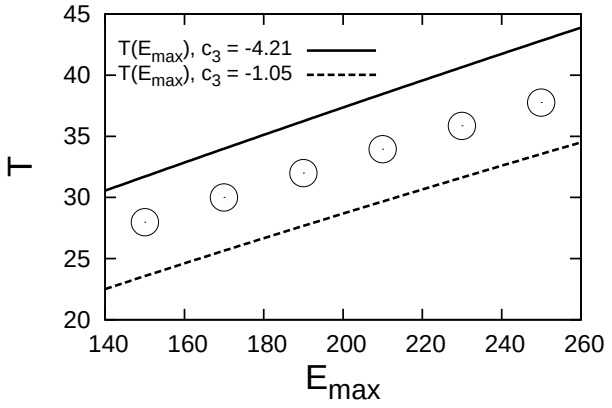

FIG. 5: Temperature as a function of the high energy cut-off $E_{\max}$, keeping fixed $F = 10^{-3}$, $E_{\min} = 5$ and $E_f = 36$, $\delta_f = 1$. Circles represent the results from numerical computations. The continuous and dashed lines are the prediction (8) for different values of c_3.

In the present Letter we have investigated the stationary states of a three-dimensional hard sphere gas whose single-particle distribution function is modeled by the homogeneous isotropic Boltzmann equation. In particular, we were interested in the steady nonequilibrium states in an open system condition, i.e. in the presence of a forcing and dissipation mechanisms. Using the language of wave turbulence theory we have assumed the presence of a *warm cascades* as steady distributions. These solutions are characterized by constant particle and energy fluxes superimposed on the thermodynamic Maxwell-Boltzmann distribution. Our assumption has allowed us to relate the thermodynamic quantities of the system to the characteristics of the forcing and dissipative terms of the equation.

In particular, we have been able to give an analytical relation for the temperature reached in the system as a function of the forcing and dissipative scales. One of the main results is that the temperature is independent of how much energy and particles we inject in the system but depends only on the cut-off scales and on the forcing scale. By a direct numerical integration of the Boltzmann equation we have shown that our numerical results are consistent with the aforementioned prediction.

We believe that the approach used in this Letter may open some perspectives towards understanding nonequilibrium steady states in other physical systems via analogies to cases widely studied by the wave turbulence theory.

* Electronic address: davideproment@gmail.com; URL: http://www.to.infn.it/~proment

[1] A. Kolmogorov, in *Proceedings (Doklady) Academy of Sciences, USSR* (1941), vol. 30, pp. 301–305.

[2] U. Frisch, *Turbulence: the legacy of AN Kolmogorov* (Cambridge University Press, 1995).

[3] V. E. Zakharov, Journal of Applied Mechanics and Technical Physics **6**, 22 (1965), ISSN 0021-8944, 10.1007/BF01565814, URL http://dx.doi.org/10.1007/BF01565814.

[4] V. Zakharov and N. Filonenko, in *Soviet Physics Doklady* (1967), vol. 11, p. 881.

[5] Y. Lvov, K. Polzin, and E. Tabak, Physical Review Letters **92**, 128501 (2004).

[6] S. Dyachenko, A. C. Newell, A. Pushkarev, and V. E. Zakharov, Physica D: Nonlinear Phenomena **57**, 96 (1992), URL http://www.sciencedirect.com/science/article/B6TVK-46JH21H-4G/2/b9bf3a47086f6f154a8c0478ca64c07b.

[7] D. V. Semikoz and I. I. Tkachev, Phys. Rev. Lett. **74**, 3093 (1995).

[8] S. Nazarenko and M. Onorato, Physica D: Nonlinear Phenomena **219**, 1 (2006).

[9] D. Proment, S. Nazarenko, and M. Onorato, Physical Review A (Atomic, Molecular, and Optical Physics) **80**, 051603 (pages 4) (2009), URL http://link.aps.org/abstract/PRA/v80/e051603.

[10] S. Galtier, S. Nazarenko, A. Newell, and A. Pouquet, Journal of Plasma Physics **63**, 447 (2000).

[11] A. Kats and V. Kontorovich, Soviet Physics-JETP **37**, 80 (1973).

[12] A. Kats, V. Kontorovich, S. Moiseev, and V. Novikov, ZhETF Pis ma Redaktsiiu **21**, 13 (1975).

[13] A. Kats, Soviet Journal of Experimental and Theoretical Physics **44**, 1106 (1976).

[14] D. Proment, M. Onorato, P. Asinari, and S. Nazarenko, ArXiv e-prints (2011), 1101.4137.

[15] C. Connaughton and S. Nazarenko, Phys. Rev. Lett. **92**, 044501 (2004).